energies

MDPI

Article

Gas Turbine Transient Performance Tracking Using Data Fusion Based on an Adaptive Particle Filter

Feng Lu [1,2,*], Yafan Wang [1], Jinquan Huang [1,2,*] and Yihuan Huang [1]

Received: 29 September 2015; Accepted: 30 November 2015; Published: 8 December 2015
Academic Editor: Terese Løvås

[1] Jiangsu Province Key Laboratory of Aerospace Power Systems, Nanjing University of Aeronautics and Astronautics, Nanjing 210016, China; yafwang@126.com (Y.W.); 18013871257@163.com (Y.H.)
[2] Collaborative Innovation Center of Advanced Aero-Engine, Beijing 100191, China
* Correspondence: lfaann@nuaa.edu.cn (F.L.); jhuang@nuaa.edu.cn (J.H.); Tel.: +86-139-5162-8575 (F.L.); +86-25-8489-5995 (J.H.); Fax: +86-25-8489-3336 (F.L. & J.H.)

Abstract: This paper considers the problem of gas turbine transient performance tracking in a cluttered environment. To increase the accuracy and robustness of state estimation, a data-fusion nonlinear estimation method based on an adaptive particle filter (PF) is proposed. This method needs local estimates transmitted to a central filtering unit for data fusion, and then global data feedback to the local PF for consensus propagation. The computational burden is shared by the local PF and central filtering unit in the data-fusion architecture. Furthermore, the PF algorithm used for the data fusion is embedded with the prior knowledge of engine health condition and adaptive to the measurement noise, and hence is called the adaptive PF. The heuristic information of state variables represented by inequality constraints tunes the local estimates by a probability density truncation method. The covariance of measurement noise is calculated by wavelet transform and utilized to update the particle importance function of the real time PF. The performance improvements of the proposed method are indicated through extensive experiments for gradual and abrupt shift performance tracking under conditions of gas turbine transient operation.

Keywords: gas turbine; performance tracking; data fusion; particle filter (PF); probability density truncation; wavelet transform

1. Introduction

Gas turbine engines provide the power for airplanes, and their reliability is vital to flight safety and performance. Nevertheless, the engine working conditions are terrible and they usually must endure high speeds, extreme temperatures and strong vibrations. Erosion and fouling of major components are unavoidable and result in a gradual deterioration of engine performance during its lifetime. Besides, foreign/domestic object damage will cause engine performance to sharply shift, and it is called an abrupt fault [1]. Engine data are periodically collected by airlines for engine health evaluation. Maintenance schedules adapted to reliable health tracking results leads to safe operation and reduced costs [2]. Hence, how to get reliable information about engine health conditions in time has drawn a lot of attention.

Engine health parameters, which are correction factors for the efficiency of the major components, are introduced to quantify the engine performance changes [3]. The engine performance tracking problem can be regarded as calculating the health parameters. Various methods such as Kalman filters (KFs), neural networks, fuzzy logic, genetic algorithms and expert systems have been proposed to obtain health parameters for engine health monitoring [3–7]. KF-based methods seem to

be the most common ones for gas turbine health estimation, but these techniques are mainly focused on engine steady state, e.g., under cruise or average conditions [8].

The engine transient condition represents how a gas turbine operates from one steady state to another steady state when the input changes. The rotating components of the engine (fan, compressor, high-pressure turbine (HPT) and low-pressure turbines (LPT)) run close to their surge boundaries during transient behavior, and some performance parameters exceed their extreme value in a short time. Generally speaking, a low-bypass engine performance anomaly more easily occurs during a transient process, e.g., acceleration and deceleration. That is to say, gas turbine transient performance tracking is more urgent compared to steady state monitoring, but up to this point in time no studies of dynamic behavior monitoring for gas turbines have been presented. This paper proposes an adaptive particle filter (PF) based data fusion approach to engine transient health monitoring.

In this paper we emphasize the problem of monitoring the health performance of key gas turbine rotating components, including fans, compressors (high-pressure compressors (HPCs)), high-pressure turbines (HPTs) and low-pressure turbines (LPTs). Failures of engine actuators, sensors, and other components are not considered. The engine performance tracking of gradual drifts and abrupt shifts during transient operation is mainly addressed, but the technique can also be applied to engine steady behavior. A data fusion architecture to monitor engine health conditions is designed, and prior knowledge of engine health state and measurement noise is utilized for a Monte Carlo simulation to tune the state estimates. The present contribution is a derivation of a data fusion method based on adaptive PF for gas turbine transient performance tracking at the theoretical, implementation and performance level.

This paper is organized as follows: Section 2 presents a review of the basic PF and the problem formulation; the adaptive PF algorithm and data fusion architecture implementation for gas turbine health monitoring is given in Section 3; the performance comparisons of the proposed method for gradual and sharp shifts in different operation conditions are discussed in Section 4; and Section 5 concludes this paper.

2. Problem Formulation and Particle Filter

2.1. Problem Formulation

A gas turbine engine is a low-bypass turbofan engine, see Figure 1. A single inlet supplies airflow to the fan. Air leaving the fan is separated into two streams: one stream passes through the engine core, and the other stream passes through the annular bypass duct and then leaves. The fan is driven by the low pressure turbine. The air passing through the engine core moves through the HPC, which is driven by the HPT. Fuel is injected in the combustor and burned to produce hot gas for driving the turbines. The gas leaves the LPT and is mixed with the air from the bypass duct through the convergent nozzle, which has a variable cross section area.

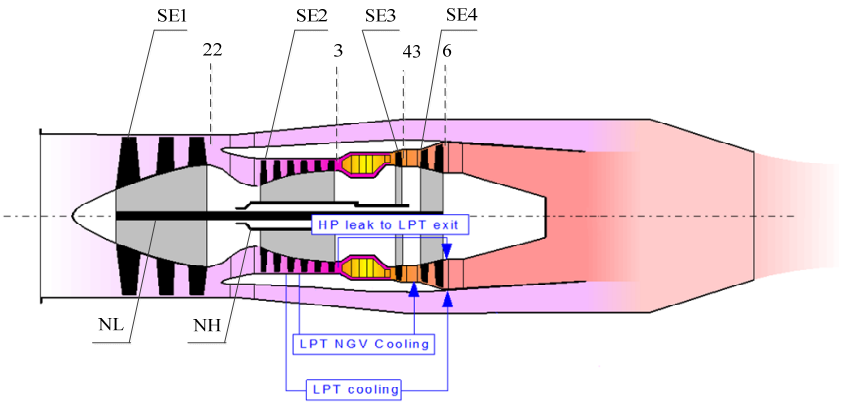

Figure 1. Schematic representation of a gas turbine engine.

Considering air flow mass, power and momentum conservation laws [9,10], a nonlinear aero-thermodynamic model of a gas turbine engine is given by:

$$\begin{aligned} x_{k+1} &= \mathrm{f}(x_k, u_k) + w_k \\ y_k &= h(x_k, u_k) + v_k \end{aligned} \tag{1}$$

where k is the time index, y is the 8-element measured output, x is the 6-element augmented state, and u is the 2-element control input. The noise terms w_k and v_k represent the process inaccuracies and measurement inaccuracies in the model. The sensor measurements are low-pressure spool speed N_{L}, high-pressure spool speed N_{H}, fan outlet pressure P_{22}, HPC outlet pressure P_3, fan outlet temperature T_{22}, HPC outlet temperature T_3, HPT outlet temperature T_{43} and LPT outlet temperature T_6. The augmented state x includes the 2-element original state x_{o} (N_{L} and N_{H}) and health parameter vector p (fan efficiency *SE1*, HPC efficiency *SE2*, HPT efficiency *SE3* and LPT efficiency *SE4*, where section efficiency is defined *SE*). The elements of the control vector in the model are fuel flow W_{f} and nozzle area A_8, which defines the engine operating point. There are two information entropy definitions used to select the system parameters. Auto Information Entropy is utilized to select the measured parameters, while the Cross Information Entropy to analyze the correlations between control, measured and health parameters.

In the framework of gas turbine performance monitoring, the quantities of interest are the differences between the estimated engine health parameters status and their reference ones. The actual engine performance is represented by the estimated values of health parameter, the prior value of which is adapted to the current measurements in a recursive approach. The block diagram of the model-based approach to monitoring the engine health condition is shown in Figure 2, and it is a closed-loop state estimator correcting structure. The KF, especially the linear KF (LKF), is an optimal state estimator for linear systems with noisy and inaccurate measurements, and is widely used for gas turbine engine health monitoring [11].

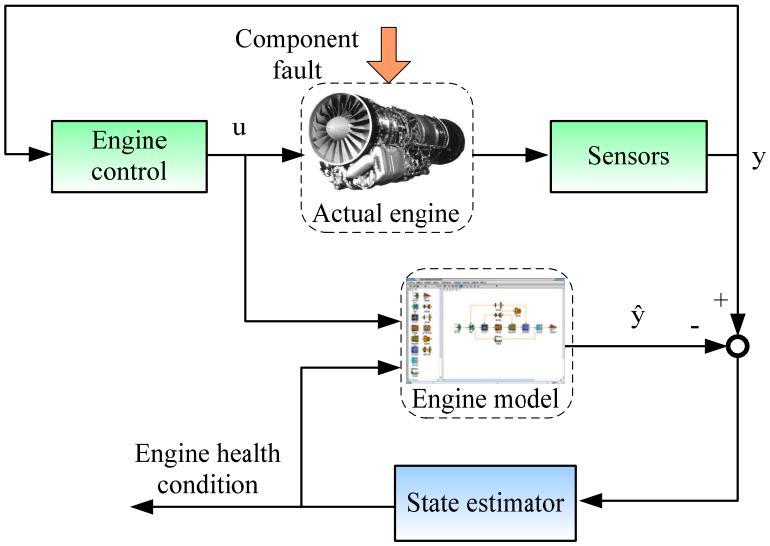

Figure 2. Gas turbine health monitoring based on a state estimator.

The state variable model (SVM) is a piecewise linear representation of the engine and needs to be established before the LKF implementation. It should be pointed out that the SVM obtained at a steady operating point is only a representation of the engine near this operating point. The state estimation accuracy by the LKF varies with the distance from the actual operating point to the design point, and also with the magnitude of the state deviation [12]. That means that the strong nonlinearity of gas turbine makes the LKF effective only in a small working range around the nominal state, and it can't do well in cases of transient behavior, e.g., during acceleration and deceleration.

Note that state variables change together in a situation of normal gradual engine deterioration, and the SVM is derived by the partial derivative calculation in the linearization process. Thus it is impossible for the SVM to correctly describe simultaneous shifts of all states, thus the tracking accuracy of gradual shifts by the LKF is not satisfactory. In addition, the assumption that the derivative of health parameter $\boldsymbol{h}$ is approximated by zero is utilized in the LKF equations, which is because engine deterioration generally occurs very slowly relative to the dynamics of the original state variables $\boldsymbol{x_0}$. Therefore any sharp shift of health parameters is not well estimated by the LKF due to the contradiction with the hypothesis $\dot{\boldsymbol{h}} = 0$. Hence, the generic LKF-based engine monitoring approach to the abrupt and multi-state gradual shift has a theoretical drawback.

To aim at the above issues, various nonlinear filtering methods are proposed and applied to state estimation, especially the extended Kalman filter (EKF), unscented Kalman filter (UKF) and PF [13,14]. Nevertheless, the EKF method is often used for weak nonlinear Gaussian systems due to a Taylor Series expansion truncated to the first order [8], and the performance closely depends on how often Jacobians are updated. Compared to the EKF and UKF, the PF is based on sequential Monte Carlo sampling theory, and it does not necessitate simplification of nonlinearity or any hypothesis of specific distributions [15,16]. Therefore, the PF-based approach is the one of the best ways that we address strongly nonlinear engine health monitoring issues in the following section.

2.2. The Particle Filter

The nonlinear model of a gas turbine is given by Equtaion (1), and let $x_{0:k} \triangleq \{x_0, \cdots, x_k\}$ and $y_{1:k} \triangleq \{y_1, \cdots, y_k\}$ denote the series of the state and measurement. Assume the probability density function (PDF) of the prior condition is $p(x_0)$, and the posterior PDF $p(x_{0:k}\,|y_{1:k}\,)$ is characterized by a set of weighted random samples $\{x^i_{0:k}, w^i_k\}^N_{i=1}$, wherein N_s is the particle number. The particle set $\{x^i_{0:k}; i = 0, \cdots, N\}$ is associated to the weights $\{w^i_k; i = 0, \cdots, N\}$, and the PDF at time k can be approximated by:

$$\begin{aligned} p(x_{0:k}\,|y_{1:k}\,) &\approx \sum_{i=1}^{N} w^i_k \delta(x_{0:k} - x^i_{0:k}) \\ \sum_{i=1}^{N} w^i_k &= 1 \end{aligned} \tag{2}$$

The case that the particles for Monte Carlo sampling are directly generated from the posterior PDF $p(x_{0:k}\,|y_{1:k}\,)$ is expected, but it is generally unavailable. Thus the importance sampling distribution function $q(x_{0:k}\,|y_{1:k}\,)$ is defined before sampling:

$$\begin{aligned} q(x_k|x_{0:k-1}, z_{1:k}) &= q(x_k|x_{k-1}, z_k) \\ q(x^i_k\Big|x^i_{k-1}, z_k) &= p(x^i_k\Big|x^i_{k-1}) \end{aligned} \tag{3}$$

Then the i^{th} particle weight w^i_k can be approximated by:

$$w^i_k \propto \frac{p(x_{0:k}\,|y_{1:k}\,)}{q(x_{0:k}\,|y_{1:k}\,)} \propto \frac{p(y_k\,|x^i_k\,)p(x^i_k\Big|x^i_{k-1})p(x^i_{0:k-1}\,|y_{1:k-1}\,)}{q(x^i_k\Big|x^i_{0:k-1}, y_{1:k})q(x^i_{0:k-1}\,|y_{1:k-1}\,)} = w^i_{k-1}\frac{p(y_k\,|x^i_k\,)p(x^i_k\Big|x^i_{k-1}\,)}{q(x^i_k\Big|x^i_{0:k-1}, y_{1:k}\,)} \tag{4}$$

With this choice and normalization, the importance weights can be computed:

$$\begin{aligned} w^i_k &\propto w^i_{k-1} p(y_k|x^i_k) \\ w^i_k &= w^i_k / \sum_{i=1}^{N} w^i_k \end{aligned} \tag{5}$$

One problem of the basic PF algorithm is that more particles have negligible weights after a few recursive steps. This implies that particle degeneracy occurs and a large computational effort for updating particle is meaningless. A typical method for solving this issue is importance re-sampling,

and each particle is assigned by equal weight $w_k^i = 1/N$ whenever the effective number N_{eff} of particles becomes less than a threshold value N_{th}.

$$N_{\text{eff}} = \frac{1}{\sum_{i=1}^{N} \left(w_k^i\right)^2} < N_{\text{th}} \tag{6}$$

Once N_{th} is close to value $N_{\text{eff},k}$, all particles have almost the same significance.

The architecture of a conventional PF mentioned above is that the measured data from different sensors are sent to one central PF to process together, and this is so-called the central architecture [15,17]. The advantage of this architecture is minimal information loss, but it also raises the problems that all measurements are identically treated at a time and the central filter bears a heavy computational burden, especially in the framework of the PF [18–20]. With the development of information fusion, the fusion PF structure employing a bank of local PFs and one master filter is presented and the computational effort is then shared by several filters [21,22].

In the case of the model-based approach to gas turbine health monitoring, the heuristic health knowledge is usually ignored and not considered in estimate algorithms. The typical anomaly modes and gradual deterioration rules of the engine have been summarized, and the magnitude ranges of health parameters are then determined. This prior knowledge about health parameters is represented by the constraints, and it can be used for state estimation in the PF algorithm. Furthermore, measurement noise levels vary with the order of the sensed value during the engine's dynamic operation. Generally speaking, the magnitude of sensed noise increases as the engine works at a larger operating point during the dynamic operation. Hence, it is very important for the PF to tune the estimate with the noise level in the situation of the transient behavior of the engine.

3. Adaptive Fusion Particle Filter

3.1. The Adaptive Particle Filter

3.1.1. Particle Filter with Inequality Constraints

The prior state information can be described by equality or inequality constraints in the state estimation algorithm. These constraint approaches are mainly concentrated and applied to linear systems, especially combined with a KF, which has been proved to increase performance estimation accuracy. KFs with equality constraint approaches include the moving horizon estimation and smoothly constrained KF [23]. The estimate projection and truncation methods are incorporated to inequality constraints on state estimates, and the latter one has better performance for deterioration tracking due to its handling of two-sided constraints. The nonlinear state estimation with inequality constraints is more useful to gas turbine engine health monitoring, but there are not enough theoretical studies. For a nonlinear dynamic system, the heuristic knowledge represented by inequality constraints is introduced to the PF algorithm. This idea based on a previously published method [24] has been extended to the nonlinear PF approach for abrupt shift tracking.

The prior information we used in this paper is derived from the gradual deterioration rule and abrupt fault feature. Engine performance degrades with use, and the health parameters never improve and change in one way. For example, we know that the health parameter representing engine efficiency declines over time, and the parameter usually varies within the -10% magnitude due to abrupt faults. With this information, we can determine the bound of the state in advance and it is represented by the inequality constraint of the state estimator. The probability density function (PDF) of the PF estimate at the prior inequality constraint is truncated and the constrained filter estimate as the mean of the truncated PDF is calculated. Now consider the nonlinear system of Equation (1) where the s scalar constraints are added:

$$a_{k,m} \leqslant \phi_{k,m}^{\mathrm{T}} x_k \leqslant b_{k,m}, \qquad m = 1, \cdots, s \tag{7}$$

where $a_{k,m} \leqslant b_{k,m}$, $a_{k,m}$ and $b_{k,m}$ are the two sided constraint of the m^{th} health parameter at time k. The health parameter estimate $\hat{x}_k$ and covariance P_k is derived by the unconstraint PF algorithm:

$$\begin{aligned} \hat{x}_k &= \sum_{i=1}^{\mathrm{N}} w_k^i x_k^i \\ P_k &= \sum_{i=1}^{\mathrm{N}} w_k^i (x_k^i - \hat{x}_k)(x_k^i - \hat{x}_k)^{\mathrm{T}} \end{aligned} \tag{8}$$

The PF algorithm with inequality constraints is to truncate the unconstrained PDF, N (x_k, P_k). Once the mean $\widetilde{x}_k$ and covariance $\widetilde{P}_k$ of the truncated PDF are computed, we can obtain the constrained health parameter estimate. The state estimate $\widetilde{x}_{k,m}$ and covariance $\widetilde{P}_{k,m}$ are defined after the first m scalar constraints enforced, and then the new transformation is performed:

$$\begin{aligned} z_{k,m} &= S_m W_m^{-\frac{1}{2}} T_m^{\mathrm{T}} (x_k - \widetilde{x}_{k,m}) \\ T_m W_m T_m^{\mathrm{T}} &= \widetilde{P}_{k,m} \\ S_m W_m^{\frac{1}{2}} T_m^{\mathrm{T}} f_{k,m} &= \begin{bmatrix} (f_{k,m}^T \widetilde{P}_{k,m} f_{k,m}^{\frac{1}{2}}) & 0 & L & 0 \end{bmatrix}^{\mathrm{T}} \end{aligned} \tag{9}$$

where T_m is orthogonal, W_m is diagonal (these two quantities, T_m and W_m, can be derived from the Jordan canonical decomposition of $\widetilde{P}_{k,m}$) and S_m is obtained using Gram–Schmidt orthogonalisation. The first m inequality constraints are normalized:

$$\begin{aligned} c_{k,m} &\leqslant [1 \quad 0 \quad 0 \cdots 0] z_{k,m} \leqslant d_{k,m} \\ c_{k,m} &= \frac{a_{k,m} - {\phi_{k,m}}^{\mathrm{T}} \widetilde{x}_{k,m}}{\left({\phi_{k,m}}^{\mathrm{T}} \widetilde{P}_{k,m} \phi_{k,m}\right)^{1/2}} \\ d_{k,m} &= \frac{b_{k,m} - {\phi_{k,m}}^{\mathrm{T}} \widetilde{x}_{k,m}}{\left({\phi_{k,m}}^{\mathrm{T}} \widetilde{P}_{k,m} \phi_{k,m}\right)^{1/2}} \end{aligned} \tag{10}$$

Since $z_{k,m}$ is an identity covariance with statistically independent element, only the first element is constrained in Equation (10), and the PDF truncation reduces to a one-dimensional PDF. The part outside of the constraints is removed due to the fact $z_{k,m}$ lays between $c_{k,m}$ and $d_{k,m}$. The truncated PDF is normalized after computing the area of the inside portion of the PDF. The mean μ_m and variance ${\sigma^2}_m$ of the first element of $\widetilde{z}_{k,m}$ with the constraint enforcement are expressed by:

$$\begin{aligned} \alpha &= \frac{\sqrt{2}}{\sqrt{\pi}(\mathrm{erf}(d_{k,m}/\sqrt{2}) - \mathrm{erf}(c_{k,m}/\sqrt{2}))} \\ \mu_m &= \alpha \textstyle\int_{c_{k,m}}^{d_{k,m}} \xi \exp(-\xi^2/2) \mathrm{d}\xi = \alpha[\exp(-c_{k,m}^2/2) - \exp(-d_{k,m}^2(k)/2)] \\ {\sigma^2}_m &= \alpha \textstyle\int_{c_{k,m}}^{d_{k,m}} (\xi - \mu_m)^2 \exp(-\xi^2/2) \mathrm{d}\xi \\ &= \alpha[\exp(-c_{k,m}^2/2)(c_{k,m} - 2\mu_m) - \exp(-d_{k,m}^2/2)(d_{k,m} - 2\mu_m)] + \mu_m^2 + 1 \end{aligned} \tag{11}$$

where α is a magnification factor. The inverse transformation of the Equation (9) is taken, and the mean and variance of the constrained state estimate are therefore given as:

$$\begin{aligned} \widetilde{x}_{k,m+1} &= T_m W_m^{1/2} S_m^{\mathrm{T}} z_{k,m+1} + \widetilde{x}_{k,m} \\ \widetilde{P}_{k,m+1} &= T_m W_m^{1/2} S_m^{\mathrm{T}} \widetilde{C}_{k,m+1} S_m W_m^{1/2} T_m^{\mathrm{T}} \end{aligned} \tag{12}$$

We repeat the process of Equations (9)–(12) to enforce the next constraint to the state estimate and jump out of the iteration until $m = s$. Hence, we obtain the state estimate and covariance at time k as $x_k = \widetilde{x}_{k,s}$, $P_k = \widetilde{P}_{k,s}$ by the constrained PF algorithm.

3.1.2. Measure Noise Tuned Particle Filter

As we know, particle importance weight w_i is closely dependent on the distance between the real sensed value and its estimate, and the smaller the distance, the larger the weight. In the basic PF algorithm, the particle importance weight w_i is defined as follows:

$$w_i = \frac{1}{\sqrt{2\pi}\sigma}\exp(-\frac{(y-\hat{y}_i)^2}{2\sigma^2}) \tag{13}$$

where the quantity σ is consistent with the covariance of measurement noise due to the fact that the sensed noise usually is generally recognized as Gaussian white noise. We set the quantity σ by the heuristic experience of the noise and it remains constant in the conventional PF algorithm. However, the probability distribution of the sensed noise changes in engine transient behavior, and it raises the problem of measurement noise uncertainty with regards to state estimation. The deviation from the actual measurement noise will result in a decline in estimation accuracy. In the paper the on-line tuning quantity σ of the PF with the measurement noise variance with the help of the wavelet transform is designed.

The measured stream $y_\omega(k)$ could be approximated by a low-order polynomial or a piecewise low-order polynomial in an observation interval [25]. This interval size is corresponding to sampling number. Suppose the polynomial of the sensed stream $y_\omega(k)$ is described as follows:

$$y_\omega(k) = a_0 + a_1 k + \cdots + a_M k^M + \omega \tag{14}$$

Then the wavelet transform is implemented to the sensed stream $m_w(k)$:

$$\begin{aligned} W_{y_\omega}(s,\tau) &= y_\omega(k) * \varphi_{s,\tau}(k) = W_y(s,\tau) + W_\omega(s,\tau) \\ \varphi_{s,\tau}(k) &= \frac{1}{\sqrt{s}}\varphi(\frac{k-\tau}{s}) \end{aligned} \tag{15}$$

where $\phi(k)$ is a wavelet function, "*" is the convolution operation, $W_y(s,\tau)$ is an approximate part of the wavelet coefficients and $W_\omega(s,\tau)$ represents a detailed part of the wavelet coefficients. We define a vanishing moment α of the function $\phi(k)$, and the measurement noise part is extracted from the sensed stream part once the quantity α is greater than the highest-order of the polynomial, namely $\alpha > M$. Then the standard deviation of the noisy term in an interval can be calculated by the following expression:

$$\sigma = \frac{1}{M}\mathrm{Med}(\left|W_{y_\omega}(s,t_\mathrm{h})\right|) \tag{16}$$

where the scale s equals to 0.5, and the series $W_{y_\omega}(s,t_\mathrm{h})$ is the $K/2$ wavelet coefficients of $\{y_\omega(k)\,|k = 0,1,\cdots K\}$, wherein $0 \leqslant h \leqslant K/2$. Normalizing parameter M is usually set at 0.6745, and the function Med() represents the middle value calculation of a series.

In order to tune the quantity σ of the PF algorithm in real-time during the engine dynamic behavior, the measurement noise of a series in an interval is computed by a wavelet transformation. The sensed stream y_ω is segmented by a window with fixed width L, and it slides forward along the sampling time. The variance of the sensed noise part in the sliding window is estimated, therefore, the framework of the adaptive PF algorithm is established as shown in Figure 3.

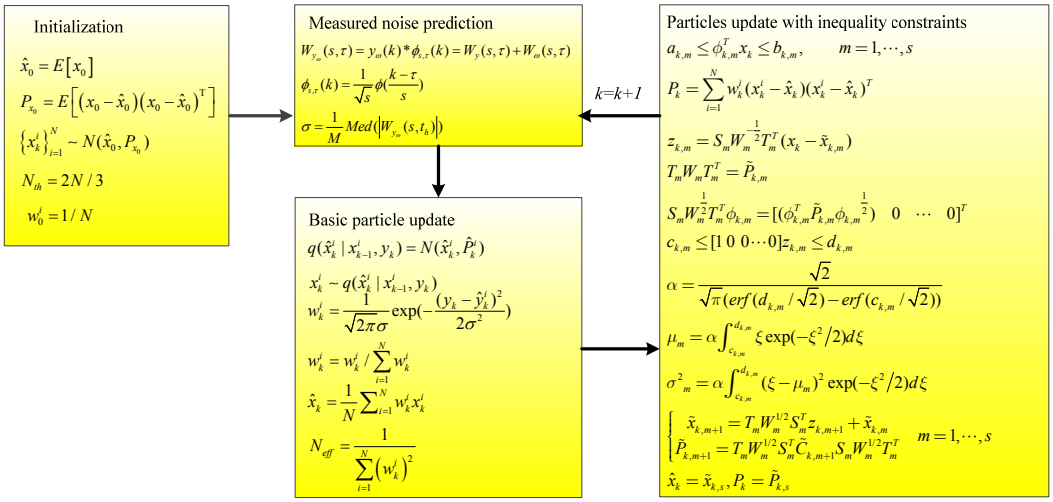

Figure 3. The framework of the adaptive particle filter (PF) algorithm.

3.2. Data Fusion Based on Adaptive Particle Filter

The fusing PF based on the integration of adaptive PF algorithm and information fusion theory is proposed for gas turbine transient performance monitoring. The sensor used to detect engine health condition is divided into several teams, and each team is applied to estimate the local estimates by the local PF. The engine component layout and thermodynamics of operation are taken into account for the partitions of local filters in the fusion architecture. The fan of the engine is a cold and low pressure (LP) component, the compressor is a cold and high pressure (HP) one, HPT is a hot and HP one, and LPT is a hot and LP one [26,27]. Two different ways to partitioning are performed, namely, the cold-hot component partition and the LP-HP component partition. Therefore, there are four combinations of the four rotating components above, which are the cold group, the hot group, the HP group and the LP group. For example, the cold partition includes two components (fan and compressor). Likewise, the hot partition consists of HPT and LPT, the HP partition of compressor and HPT, and the LP partition of fan and LPT.

For the cold group, the measured parameters are T_{22}, P_{22}, T_3 and P_3. In a similar manner the measurements T_{43} and T_6 are for the hot group, the sensors T_{22}, P_{22} and T_6 for the LP group, and the sensors T_3, P_3, and T_{43} for the HP group. In addition, two spool speeds (N_L and N_H) are important quantities representing engine operation status, which are communal measurements and utilized in each part. Hence, the measurements of four local filter can be denoted by $y_1 = [N_L, N_H, T_{22}, P_{22}, T_3, P_3]$, $y_2 = [N_L, N_H, T_{43}, T_6]$, $y_3 = [N_L, N_H, T_{22}, P_{22}, T_6]$, $y_4 = [N_L, N_H, T_3, P_3, T_{43}]$. Although the measurements of each engine component partition are different, the health parameters to be estimated are the same in every local filter, namely, *SE1*, *SE2*, *SE3* and *SE4*.

The data fusion estimation based on the adaptive PF mainly includes three stages. First, several local filters perform in parallel to obtain individual sensor-based estimates. Second, all local estimates are combined in a master filter, where a global state estimate is yielded. Third, the global state and covariance is fed back to local filters with an information- sharing strategy for next cycle. The procedure of data fusion for the engine transient performance estimation is summarized as follows:

Step 1: Initialization

Given the initial values of global state x_0, estimation error covariance P_0, and process noise covariance Q_0 in the master filter. The four local filters are initialized with the information allocation strategy:

$$Q_{j,0} = \beta_j^{-1} Q_{m,0} \quad P_{j,0} = \beta_j^{-1} P_{m,0} \quad X_{j,0} = \beta_j^{-1} X_{m,0} \quad j = 1, \cdots, 4 \tag{17}$$

where the information distribution factor β_j follows:

$$\sum_{j=1}^{4} \beta_j = 1 \tag{18}$$

Step 2: The adaptive PF performs in the local filter.

The particles $\{x^i_{j,0:k-1}, w^i_{j,k-1}\}^{N}_{i=1}$ are generated based on the prior distribution $N(X_{j,k-1}, P_{j,k-1})$, and are propagated through the nonlinear model Equation (1). The numerical characteristics of the measured noise are computed by wavelet transformation, and the quantity σ is applied to the importance weight calculation. The known health information is imposed to the PF to produce the local constrained estimates of the state $\hat{x}_{j,k}$, error covariance $\hat{P}_{j,k}$ and noise covariance $Q_{j,k}$.

Step 3: Information fusion implements in the master filter.

The local estimates $\hat{x}_{j,k}$, $\hat{P}_{j,k}$, and $Q_{j,k}$ are sent to the master filter to fulfill the information fusion for the global optimal estimate $x_{m,k}$. The estimate error covariance $\hat{P}_{j,k}$ is an important parameter representing the performance of the local filter, and it is used to calculate the fusing weight of the local filter. The larger the covariance $\hat{P}_{j,k}$ is, the smaller the fusing weight in the global state is in the paper:

$$\begin{aligned} Q_{m,k} &= (\sum_{j=1}^{4} {Q_{j,k}}^{-1})^{-1} \\ P_{m,k} &= (\sum_{j=1}^{4} \hat{P}_{j,k}^{-1})^{-1} \\ x_{m,k} &= P_{m,k} \times \sum_{j=1}^{4} \hat{P}_{j,k}^{-1} x_{j,k} \end{aligned} \tag{19}$$

Step 4: Information distribution strategy

The state estimate calculated by the master filter is transmitted back to each local filter with an information assignment strategy:

$$Q_{j,k} = \beta_j^{-1} Q_{m,k} \quad P_{j,k} = \beta_j^{-1} P_{m,k} \quad X_{j,k} = X_{m,k} \quad j = 1 \cdots N \tag{20}$$

Due to the fact that information distribution factor β_j has no effect on estimation accuracy, it is set by $\beta_j = \dfrac{1}{N}$.

Steps (2)–(4) present the fusing PF algorithm at iteration k. For iteration $k + 1$, the state and covariance delay a time index and Steps (2)–(4) are repeated. The fusion filter architecture is shown in Figure 4 for gas turbine transient performance estimation.

As shown in the figure, we can see that calculation loads are shared both by the local filters, and the master filter no longer undertakes the whole process like in the basic PF algorithm. Since the time update and measurement update are carried out independently in every local filter, the individual estimate by the local filter is not immediately affected by others. In the gas turbine engine health monitoring application, the data fusion filter architecture has a more efficient capability to deal with state estimation in cases of sensor fault due to fusing weight adaptive to estimation accuracy of the local filter.

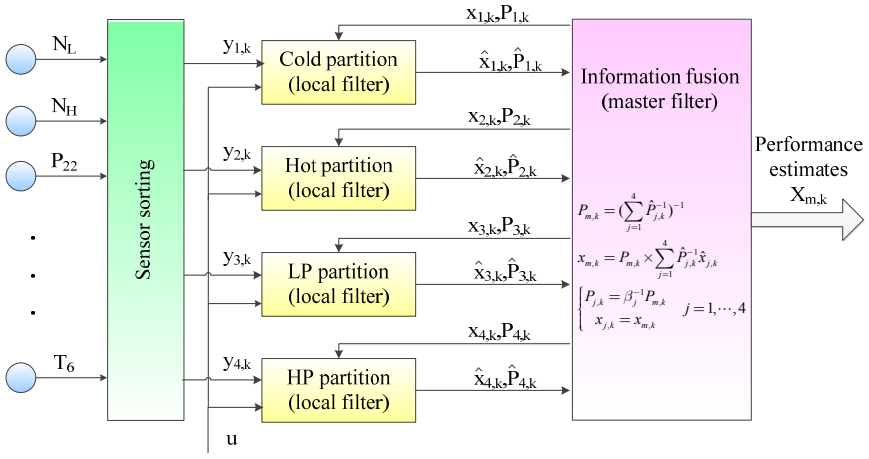

Figure 4. Data fusion filter architecture for gas turbine performance estimation.

4. Simulation and Analysis

The data fusion based on the adaptive PF approach is evaluated for the engine performance monitoring using the Matlab software. In the simulation environment, we use the component-level-model (CLM) engine to take the place of the actual engine, and the sampling rate equals to 50 Hz. The hardware of computer used for simulation is configured as follows: CPU i3-2100 @ 3.10 GHz and RAM 2GB. The standard deviations of measurement and health parameter are shown in Tables 1 and 2. Gaussian noise v with magnitude specified in Table 1 is added to the simulated measured values, and the independent system noise and initial measured noise separately follow $\omega \sim N(0, Q)$ and $v \sim N(0, R)$, wherein $Q = 0.16 \times 10^{-4} I_{6\times 6}$.

Table 1. Gas turbine component-level-model (CLM) model measurements, nominal value and standard deviation. High-pressure compressor: HPC; high-pressure turbine: HPT; low-pressure turbine: LPT.

Measurement	Acronyms	Normalized Value	Standard Deviation
Low pressure spool speed	N_L	1	0.0015
High pressure spool speed	N_H	1	0.0015
Fan outlet temperature	T_{22}	1	0.002
Fan outlet pressure	P_{22}	1	0.0015
HPC outlet temperature	T_3	1	0.002
HPC outlet pressure	P_3	1	0.0015
HPT outlet temperature	T_{43}	1	0.002
LPT outlet temperature	T_6	1	0.002

Gas turbine health condition is represented by health parameters as mentioned in the previous section. Table 2 shows four abrupt faults representative of possible situations expected to be encountered in practice, and the health parameter deviation in each case refers to lab record of the Rolls-Royce Company (London, UK) [3,28]. For example, Case 1 is a fan abrupt fault with its efficiency *SE1* deviating 1%. Assume that there are no fault on sensor measurements in the following experiments.

Table 2. Gas turbine engine abrupt fault modes and their deviation.

Scenarios	Acronyms	Fault Mode	Deviation	Standard Deviation
Case 1	*SE1*	Fan abrupt fault	−1% on *SE1*	0.0005
Case 2	*SE2*	HPC abrupt fault	−1% on *SE2*	0.0005
Case 3	*SE3*	HPT abrupt fault	−1% on *SE3*	0.0005
Case 4	*SE4*	LPT abrupt fault	−1% on *SE4*	0.0005

Engine gradual deterioration due to normal usage is simulated by linear drift of four health parameters, beginning from a healthy engine (the four parameters equal to 1) at cycle number $n = 0$ and with the degeneration at the end of the sequence at $n = 6000$: -2.18% on *SE1*, -6.71% on *SE2*, -3.22% on *SE3* and -0.81% on *SE4*. Considering the magnitude of both the engine abrupt fault and deterioration, the bounds of the health parameter representing the PF inequality constraints are separately set by $a = [1.005,1.005,1.005,1.005]^{\mathrm{T}}$ and $b = [0.97,0.90,0.96,0.98]^{\mathrm{T}}$. The performance of the engine anomaly detection is assessed by three indices, namely, root-mean-square error (*RMSE*), convergence time and root-mean-square deviation (*RMSD*). The *RMSE* and *RMSD* are separately defined by:

$$\begin{aligned} RMSE &= [\frac{1}{S}\sum_{i=1}^{S}(\hat{x}_i - x_i)^2]^{\frac{1}{2}} \\ RMSD &= [\frac{1}{S}\sum_{i=1}^{S}(\hat{x}_i - \overline{\hat{x}}_i)^2]^{\frac{1}{2}} \end{aligned} \tag{21}$$

where S is the sampling step and $\overline{\hat{x}}_i$ the mean of estimate value. The convergence time T_c is used to indicate the delay in fault recognition. We define this time index in this paper that is from the starting deviation to the estimate steady state within $\pm 0.02\%$ range and no longer out of this range in two consecutive steps.

4.1. Abrupt Fault Diagnosis in Steady Operation Conditions

The tests on gas turbine abrupt fault diagnosis are first performed at ground steady conditions ($H = 0$ m, $Ma = 0$, $W_f = 2.48$ kg/s). The abrupt faults depicted in Table 2 are simulated, and the noise is not changed in the engine steady behavior. Given the stochastic character of the measurement noise, each test-case has been run five times. Then the engine fault diagnostic performances of basic KF, basic PF, fusion particle filter (F-PF) and fusion adaptive particle filter (FA-PF) are given in Table 3. The particle number of the PF is 60, and that of both the F-PF and FA-PF is 30.

The *RMSE*s and *RMSD*s of the two fusion PF approaches shown in Table 3 are smaller than those of the conventional PF and KF in the cases of the four abrupt fault modes, and the FA-PF one is superior to the others. The convergence time of the three PF approaches are nearly the same, and vary clearly in different cases. The KF is a linear estimator and it takes less time to reach the steady state. Two speed measurements are repeatedly utilized in each local filter and there is the reason for the fact the importance of their weights is increasing compared to the remaining measurements in the fusion filter structure. The fusion PF approaches have more satisfactory estimation accuracy due to sufficient extraction and information-sharing of key measurements such as the speeds for health monitoring. Because of the heuristic health knowledge enforced through inequality constraints, the FA-PF has the best estimation accuracy of fault diagnosis in the engine steady operation.

Table 3. The engine fault diagnostic performances of four filtering approaches in steady behavior. Kalman filter: KF; fusion particle filter: F-PF; fusion adaptive particle filter: FA-PF.

Fault Modes	Root-Mean-Square Error (*RMSE*)				Root-Mean-Square Deviation (*RMSD*)				T_c (ms)			
	KF	PF	F-PF	FA-PF	KF	PF	F-PF	FA-PF	KF	PF	F-PF	FA-PF
Case 1	0.0141	0.0108	0.0073	0.0059	0.0090	0.0085	0.0052	0.0044	220	190	230	220
Case 2	0.0137	0.0111	0.0078	0.0057	0.0094	0.0089	0.0059	0.0047	260	440	420	440
Case 3	0.0113	0.0118	0.0087	0.0060	0.0093	0.0096	0.0061	0.0050	320	620	660	600
Case 4	0.0126	0.0115	0.0080	0.0067	0.0100	0.0091	0.0058	0.0051	460	680	760	640

4.2. Abrupt Fault Diagnosis in Dynamic Operation

In order to further evaluate the proposed method performance in engine transient performance tracking, more simulation is carried out in the case of mixed gradual deterioration and abrupt faults. Gradual deterioration refers to all health parameters degrading linearly from the healthy condition

to the end of 3000 cycles, and a simulated abrupt fault of magnitude −1% is added to *SE2* at 5 s. The engine operates in the dynamic behavior mode from W_f = 2.48 kg/s to 1.98 kg/s under three operation conditions: ground (H = 0 m, Ma = 0), high-altitude 1 (H = 8000 m, Ma = 0.5), and high-altitude 2 (H = 11000 m, Ma = 0.8). The particle number of the three PFs is set the same as previously, and the measurement noises remain unchanged. A comparison of the three approaches for the engine transient performance tracking in the cases of mixing gradual deterioration and abrupt fault at ground is depicted in Figure 5, where the dotted line and solid line are the real and estimated values of health parameters, respectively.

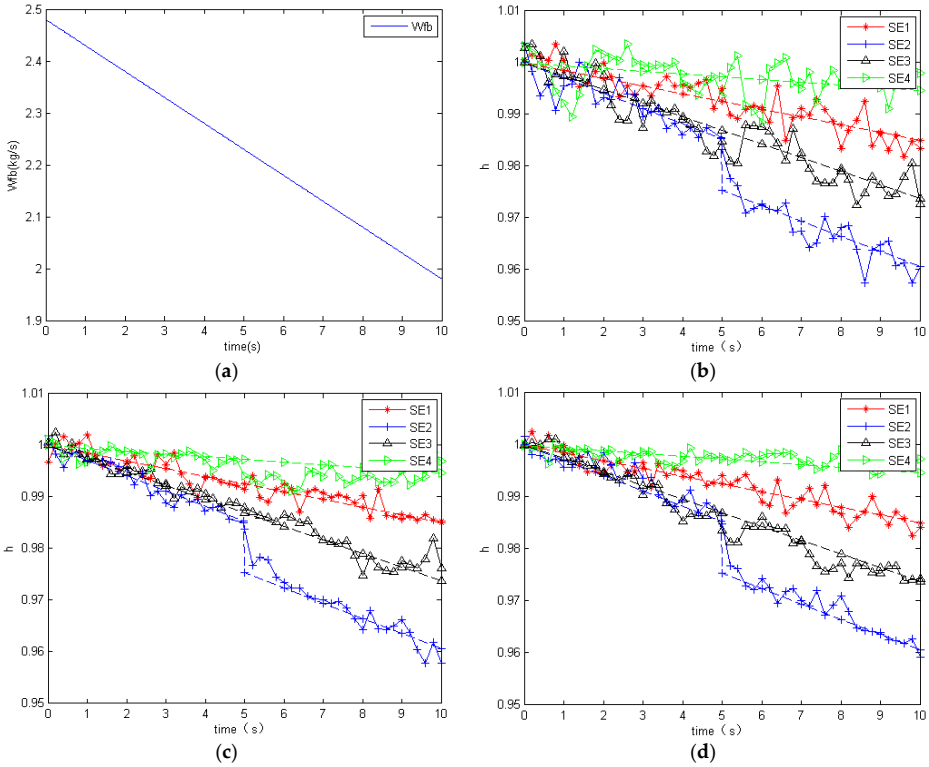

Figure 5. Engine transient performance tracking at ground condition. (**a**) Fuel supply rule W_f; (**b**) the performance estimates by the PF; (**c**) the performance estimates by the F-PF; and (**d**) the performance estimates by the FA-PF.

It can readily be found from the Figure 5 that the PF working in fusion architecture outperforms the basic PF. Table 4 further presents the estimation performance by the three PF methods in terms of number and data at different operating conditions. As can be seen from Table 4, the *RMSE* of the F-PF and FA-PF is smaller than that of PF, among which the FA-PF in three operation conditions are below 0.007. Hence, the estimation accuracy of fusion PF architecture outperforms that of the generic PF structure.

Table 4. The *RMSE* of dynamic estimation at three operation conditions.

Operation Condition	PF	F-PF	FA-PF
Ground	0.0120	0.0077	0.0069
High-altitude 1	0.0124	0.0076	0.0069
High-altitude 2	0.0123	0.0079	0.0070

4.3. Performance Estimation with Uncertain Noise in Dynamic Operation

The stochastic feature of the engine measured noise changes at different operation points. An experiment of gradual deterioration tracking with uncertain measurement noise is performed to

assess the FA-PF algorithm. The engine experiences dynamic operation in the case of gradual deterioration as the same as the Section 4.2, but no abrupt fault is added. A series of the tests are implemented with ground conditions, including the change of only one measurement noise and all measurement noises simultaneously. Noise generated in the engine core, by sources such as the HPC, combustor, HPT and LPT, plays the most important roles to the overall noise under low-power conditions. While jet and fan noises have dominated over core noise at high engine power during takeoff [29].

The sensor noise varies with engine power condition in transient process. The uncertain noise of one sensor P_{22} in Figure 6 is simulated by the route of R_0 = diag[0.0015, 0.0015, 0.002, 0.0015, 0.002, 0.0015, 0.002, 0.002] in 0–3 s, R_1 = diag[0.0015, 0.0015, 0.002, 0.003, 0.002, 0.0015, 0.002, 0.002] in 3.02–6 s and R_2 = diag[0.0015, 0.0015, 0.002, 0.0045, 0.002, 0.0015, 0.002, 0.002] in 6.02–10 s. The uncertain noise of each measurement undertakes the varied noise by R_0 in 0–3 s, $2R_0$ in 3.02–6 s, and $3R_0$ in 6.02–10 s in Figure 7. The size of the sliding window by wavelet transform is 50 steps.

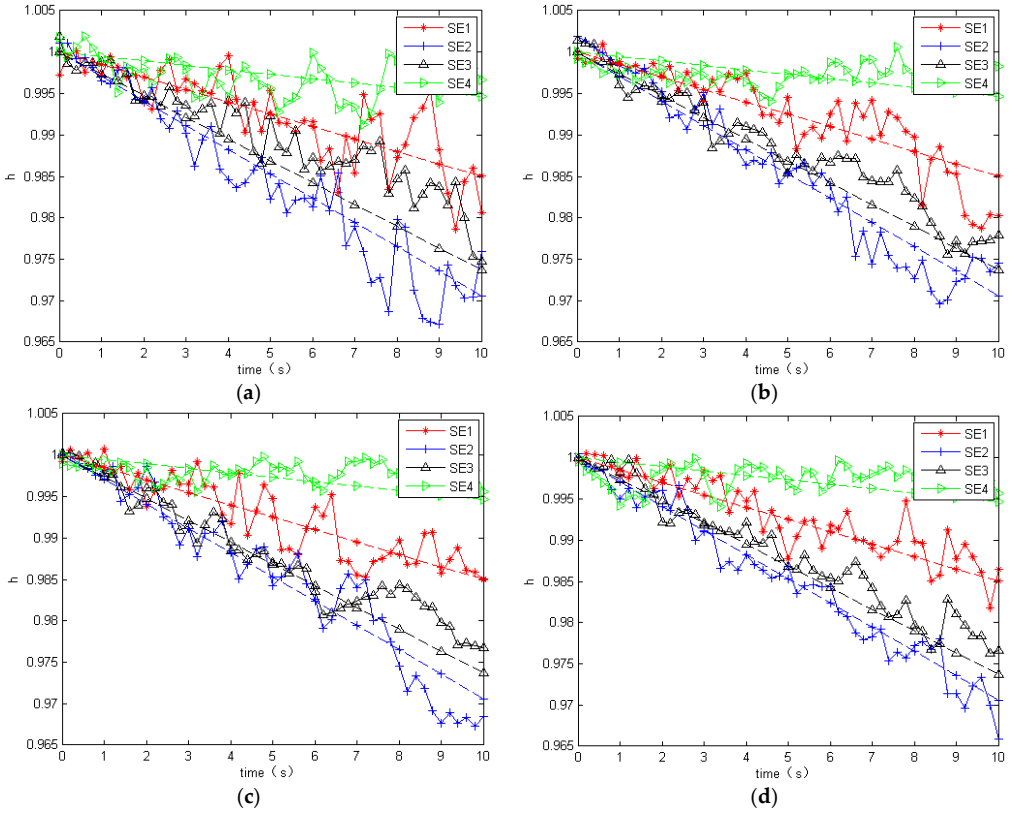

Figure 6. Transient performance monitoring with uncertain noise of one sensor P_{22} in the case of gradual deterioration. (**a**) σ = R_0; (**b**) σ = R_1; (**c**) σ = R_2; and (**d**) adaptive σ.

As shown in Figure 6, the engine transient performance estimates by the fusion PF approaches seem to deviate from their real values once the noise of sensor P_{22} varies, no matter the quantity of measurement noise σ is equal to R_0, R_1 or R_2. The fusion adaptive PF has sound tracking performance due to the quantity σ adaptive to the real measurement noise real time in Figure 6d. We can obtain similar results in the case that all sensors for transient performance monitoring have uncertain measured noise in Figure 7.

Table 5 summarizes the *RMSE* of the engine transient health estimation performance by the fusion PF approach with different the variable σ. The covariance of the measurement noise is estimated and real time tunes the quantity σ of the FA-PF algorithm as presented previously, and the *RMSE*s of the FA-PF are almost the same as those of the fusion PF where quantity σ is equal to the true value of measurement noise covariance in Table 5. Nevertheless, if the quantity σ is not tuned to

the covariance of the real measurement noise, the fusion PF will produce a larger *RMSE* in terms of the engine transient performance estimation.

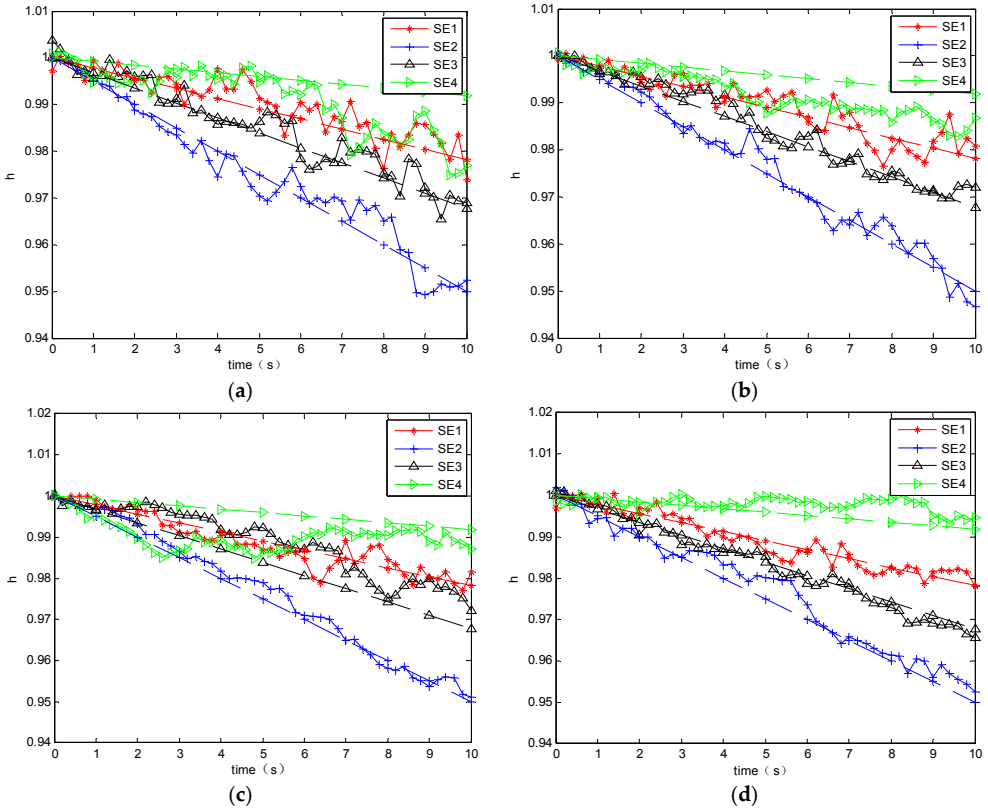

Figure 7. Transient performance monitoring with uncertain noise of every sensor in the case of gradual deterioration. (**a**) $\sigma = R_0$; (**b**) $\sigma = 2R_0$; (**c**) $\sigma = 3R_0$; and (**d**) adaptive σ.

Table 5. The *RMSE* of dynamic estimation with uncertain measurement noise at ground.

σ	Uncertain Noise of Sensor P_{22}				
	R_0	R_1	R_2	True Value	Tuning Value
RMSE	0.0121	0.0109	0.0108	0.0085	0.0088
σ	**Uncertain Noise of All Sensors**				
	R_0	$2R_0$	$3R_0$	True Value	Tuning Value
RMSE	0.0165	0.0116	0.0169	0.0095	0.0096

4.4. Engine Health Monitoring Test

Finally a test of the engine health monitoring is carried out to evaluate the proposed method at ground level. The engine input variables, W_f and A_8, are fed into the engine as shown in Figure 8. The engine *NH* representing the engine operation varies as follows: about 0.91 before 2.7 s, increasing from 0.91 to 1.0, then decreasing from 1.0 to 0.91, and about 0.91 to the end. During this process, the engine thrust increases from 0.819 to 1.0, and then back to 0.819. Four abrupt faults depicted in Table 2 are separately injected into the engine at 2 s.

Figure 9 depicts the variance estimates of measurement noise, which are applied to tune the quantity σ in the FA-PF method. The noise pollutes the true measurement, and it changes along the engine operation condition (the larger the power condition, the more noise enforcement). Table 6 summarizes the performance of engine health monitoring by four PF methods in the abrupt fault cases. The fusion PF with inequality constraints is defined by the FC-PF. The detection results

in Table 6 show that the FC-PF and FA-PF have the less estimation errors and provide more stable estimates than the other PF methods because of the prior knowledge used. Furthermore, the performance of the FA-PF for engine health monitoring is the best due to the quantity of the importance function σ adaptive to the measurement noise real-time.

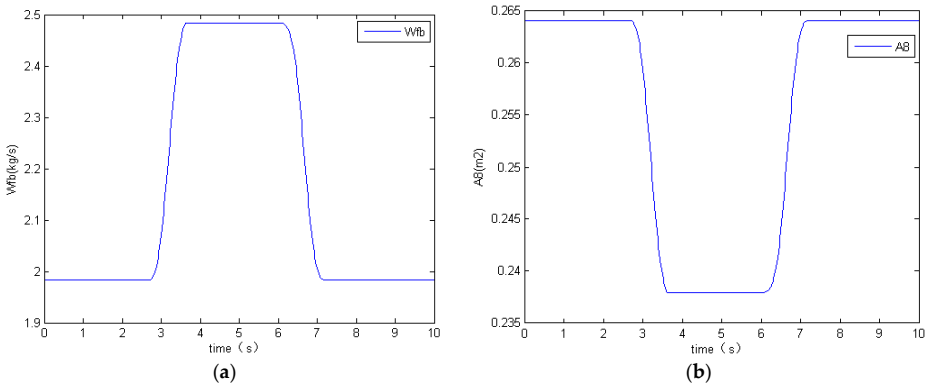

Figure 8. The change rules of the engine input variables. (**a**) W_f; and (**b**) A_8.

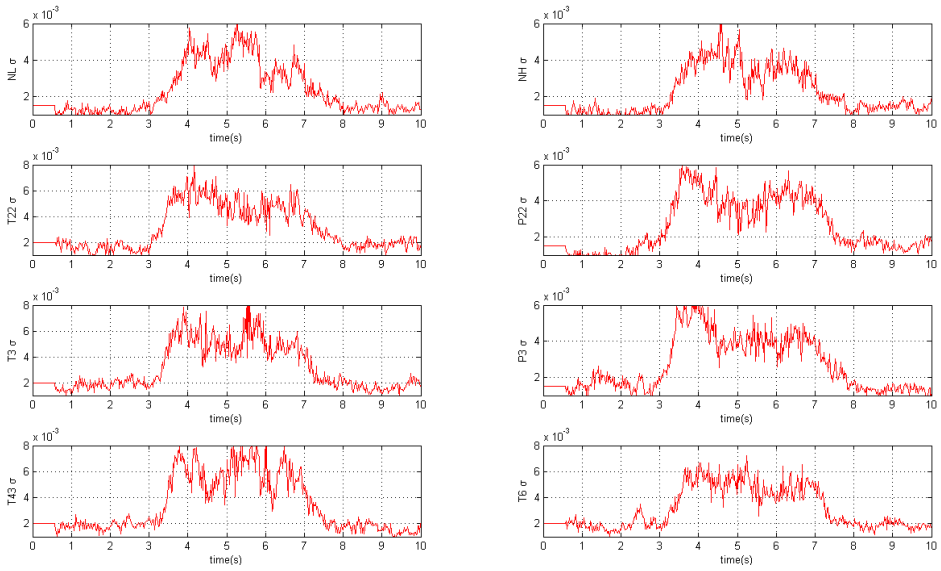

Figure 9. The variance estimates of measurement noise in the FA-PF.

Table 6. Engine health monitoring performance by four PF methods in the cases of abrupt fault.

Fault Modes	*RMSE*				*RMSD*			
	PF	**F-PF**	**FC-PF**	**FA-PF**	**PF**	**F-PF**	**FC-PF**	**FA-PF**
Case 1	0.0140	0.0101	0.0084	0.0061	0.0123	0.0083	0.0075	0.0050
Case 2	0.0138	0.0095	0.0078	0.0055	0.0119	0.0079	0.0069	0.0043
Case 3	0.0134	0.0100	0.0089	0.0058	0.0117	0.0069	0.0079	0.0050
Case 4	0.0144	0.0106	0.0094	0.0065	0.0132	0.0077	0.0079	0.0052

5. Conclusions

This paper describes the use of data fusion based on the adaptive PF for gas turbine dynamic performance monitoring. The state estimation in the fusion estimator architecture includes three steps: several local filters working in parallel to obtain individual sensor-based estimates, one master filter fusing these local estimates to yield a global state estimate, and the global estimates serving as the feedback to each local filter with information-sharing strategy. A systematic comparison of the

fusion PF methods for transient performance estimation is presented. Gradual deterioration, abrupt faults and their mixtures are typically considered as the engine anomaly scenarios in the test. The fusion PF architecture has better estimation accuracy and less convergence time than the conventional PF architecture. The implementation of the fusion PF is quite straightforward and involves only basic matrix operations. The convergence time by the fusion PF is similar to that by the basic PF, yet the computational burden of the master filter is reduced, because it is shared by local filters in the fusion PF structure.

Moreover, an adaptive PF algorithm is proposed to sufficiently utilize prior information for the engine transient performance detection with measurement noise uncertainty. The heuristic health knowledge is usually neglected in model-based engine diagnoses due to the complex mathematics application to the conventional PF. In this paper, the engine prior health information represented by the inequality constraints is enforced in the fusion PF algorithm. In addition, the uncertainty of the measurement noise in the engine dynamic operation is considered in the fusion PF. The covariance of the sensed noise is estimated and then applied to tune the importance weights of the PF. The improvements brought by the data fusion based on the adaptive PF have been illustrated on the application of the engine transient performance monitoring with noise uncertainty. The experiments show that the proposed method leads to the more reliable assessments of the engine health conditions no matter whether the cases involve gradual engine deterioration or abrupt faults. With information fusion, *a priori* knowledge and measurement noise adaption in mind, the data fusion based on the adaptive PF approach seems therefore to be more promising. The present work by the authors has shown the advantages of data fusion based on an adaptive PF for gas turbine health monitoring. It is not considered that the phase errors between different measurements combined with the senor lag will affect the shift in engine performance, and it would be interesting to discuss the proposed approach of this paper with addition of measurement differences.

Acknowledgments: We are grateful for the financial support of the National Nature Science Foundation of China (No. 61304133), the Fundamental Research Funds for the Central Universities (No. NS2015024). Moreover, the authors wish to thank the anonymous reviewers for their constructive comments and great help in the writing process, which improve the manuscript significantly.

Author Contributions: Feng Lu and Jinquan Huang contributed in developing the ideas of this research, Yafan Wang and Yihuan Huang performed this research. All of the authors were involved in preparing this manuscript.

Conflicts of Interest: The authors declare no conflict of interest.

References

1. Volponi, A. Gas turbine engine health management: Past, present, and future trends. *J. Eng. Gas Turbines Power* **2014**, *136*. [CrossRef]
2. Rodger, J.A. Toward reducing failure risk in an integrated vehicle health maintenance system: A fuzzy multi-sensor data fusion Kalman filter approach for IVHMS. *Expert Syst. Appl.* **2012**, *39*, 9821–9836. [CrossRef]
3. Borguet, S.; Léonard, O. Comparison of adaptive filters for gas turbine performance monitoring. *J. Comput. Appl. Math.* **2010**, *234*, 2202–2212. [CrossRef]
4. Li, Y.G.; Korakianitis, T. Nonlinear weighted-least-squares estimation approach for gas-turbine diagnostic applications. *J. Propuls. Power* **2011**, *27*, 337–345. [CrossRef]
5. Joly, R.B.; Ogaji, S.O.T.; Singh, R.; Probert, S.D. Gas-turbine diagnostics using artificial neural-networks for a high bypass ratio military turbofan engine. *Appl. Energy* **2004**, *78*, 397–418. [CrossRef]
6. Vanini, Z.N.S.; Khorasani, K.; Meskin, N. Fault detection and isolation of a dual spool gas turbine engine using dynamic neural networks and multiple model approach. *Inf. Sci.* **2014**, *259*, 234–251. [CrossRef]
7. Eustace, R.W. A real-world application of fuzzy logic and influence coefficients for gas turbine performance diagnostics. *J. Eng. Gas Turbines Power* **2008**, *130*. [CrossRef]
8. Simon, D. A comparison of filtering approaches for aircraft engine health estimation. *Aerosp. Sci. Technol.* **2008**, *12*, 276–284. [CrossRef]

9. Sun, J.G.; Vasilyev, V.; Ilyasov, B. *Advanced Multivariable Control Systems of Aeroengines*; Beihang Press: Beijing, China, 2005; pp. 60–83.
10. Lu, F.; Chen, Y.; Huang, J.Q.; Zhang, D.D. An integrated nonlinear model-based approach to gas turbine engine sensor fault diagnostics. *J. Aerosp. Eng.* **2014**, *228*, 2007–2021. [CrossRef]
11. Volponi, A. *Enhanced Self Tuning On-Board Real-Time Model (eSTORM) for Aircraft Engine Performance Health Tracking*; Technical Report for National Aeronautics and Space Administration: Cleveland, OH, USA, 2008.
12. Armstrong, J.B.; Simon, D.L. *Implementation of an Integrated On-Board Aircraft Engine Diagnostic Architecture*; Technical Report for National Aeronautics and Space Administration: Cleveland, OH, USA, 2012.
13. Simon, D. Kalman filtering with state constraints: A survey of linear and nonlinear algorithms. *IET Control Theory Appl.* **2010**, *4*, 1303–1318. [CrossRef]
14. Lu, F.; Huang, J.Q.; Lv, Y.Q. Gas path health monitoring for a turbofan engine based on a nonlinear filtering approach. *Energies* **2013**, *6*, 492–513. [CrossRef]
15. Gordon, N.; Salmond, D.; Smith, A. Novel Approach to Nonlinear/Non-Gaussian Bayesian State Estimation. *IEE Proc. F Radar Signal Process.* **1993**, *140*, 107–113. [CrossRef]
16. Climente-Alarcon, V.; Antonino-Daviu, J.A.; Haavisto, A.; Arkkio, A. Particle filter-based estimation of instantaneous frequency for the diagnosis of electrical asymmetries in induction machines. *IEEE Trans. Instrum. Meas.* **2014**, *63*, 2454–2463. [CrossRef]
17. Zhao, B.; Skjetne, R.; Blanke, M.; Dukan, F. Particle filter for fault diagnosis and robust navigation of underwater robot. *IEEE Trans. Control Syst. Technol.* **2014**, *22*, 2399–2407. [CrossRef]
18. Tao, G.L.; Deng, Z.L. Self-tuning fusion Kalman filter for multisensor single-channel ARMA signals with coloured noises. *IMA J. Math. Control Inf.* **2015**, *32*, 55–74. [CrossRef]
19. Zhu, H.Y.; Zhai, Q.Z.; Yu, M.W.; Han, C.Z. Estimation fusion algorithms in the presence of partially known cross-correlation of local estimation errors. *Inf. Fusion* **2014**, *18*, 187–196. [CrossRef]
20. Seifzadeh, S.; Khaleghi, B.; Karray, F. Distributed soft-data-constrained multi-model particle filter. *IEEE Trans. Cybern.* **2015**, *45*, 384–394. [CrossRef] [PubMed]
21. Zajac, M. Online fault detection of a mobile robot with a parallelized particle filter. *Neurocomputing* **2014**, *126*, 151–165. [CrossRef]
22. Li, T.C.; Sun, S.D.; Sattar, T.P. Fight sample degeneracy and impoverishment in particle filters: A review of intelligent approaches. *Expert Syst. Appl.* **2014**, *41*, 3944–3954. [CrossRef]
23. Simon, D. *Constrained Kalman Filtering via Density Function Truncation for Turbofan Engine Health Estimation*; Technical Report for National Aeronautics and Space Administration: Cleveland, OH, USA, 2006.
24. Boulkroune, B.; Darouach, M.; Zasadzinski, M. Moving horizon state estimation for linear discrete-time singular systems. *IET Control Theory Appl.* **2010**, *4*, 339–350. [CrossRef]
25. Yadav, S.K.; Sinha, R.; Bora, P.K. Electrocardiogram signal denoising using non-local wavelet transform domain filtering. *IET Signal Process.* **2015**, *9*, 88–96. [CrossRef]
26. Kyriazis, A.; Mathioudakis, K. Enhance of fault localization using probabilistic fusion with gas path analysis algorithms. *J. Eng. Gas Turbines Power* **2009**, *131*. [CrossRef]
27. Kaltungo, A.Y.; Sinha, J.K.; Elbhbah, K. An improved data fusion technique for faults diagnosis in rotating machines. *Measurement* **2014**, *58*, 27–32. [CrossRef]
28. Curnock, B. *Obidicote Project—Work Package 4: Steady-State Test Cases*; Rolls-Royce PLC: Manchester, UK, 2000.
29. Hultgren, L.S.; Miles, J.H. Noise-Source Separation Using Internal and Far-Field Sensors for a Full-Scale Turbofan Engine. In Proceedings of the 15th AIAA/CEAS Aeroacoustics Conference (30th AIAA Aeroacoustics Conference) Cosponsored by AIAA and CEAS, Miami, FL, USA, 11–13 May 2009.